

## Discovery of stars surrounded by iron dust in the LMC

ESTER MARINI,<sup>1,2</sup> FLAVIA DELL'AGLI,<sup>3,4</sup> MARCELLA DI CRISCIENZO,<sup>2</sup> SIMONETTA PUCCHETTI,<sup>5</sup>  
D. A. GARCÍA-HERNÁNDEZ,<sup>3,4</sup> LARS MATTSSON,<sup>6</sup> AND PAOLO VENTURA<sup>2</sup>

<sup>1</sup>*Dipartimento di Matematica e Fisica, Università degli Studi di Roma Tre  
Via della vasca navale 84, 00100, Roma, Italy*

<sup>2</sup>*INAF, Osservatorio Astronomico di Roma  
Via Frascati 33, 00077, Monte Porzio Catone, Italy*

<sup>3</sup>*Instituto de Astrofísica de Canarias (IAC), E-38200 La Laguna, Tenerife, Spain*

<sup>4</sup>*Departamento de Astrofísica, Universidad de La Laguna (ULL), E-38206 La Laguna, Tenerife, Spain*

<sup>5</sup>*ASI, Via del Politecnico, 00133 Roma, Italy*

<sup>6</sup>*Nordita, KTH Royal Institute of Technology and Stockholm University  
Roslagstullsbacken 23, SE-106 91 Stockholm, Sweden*

(Received January 1, 2018; Revised January 7, 2018; Accepted April 26, 2022)

Submitted to ApJ

### ABSTRACT

We consider a small sample of oxygen-rich, asymptotic giant branch stars in the Large Magellanic Cloud, observed by the *Spitzer* Space Telescope, exhibiting a peculiar spectral energy distribution, which can be hardly explained by the common assumption that dust around AGB stars is primarily composed of silicate grains. We suggest that this uncommon class of objects are the progeny of a metal-poor generation of stars, with metallicity  $Z \sim 1 - 2 \times 10^{-3}$ , formed  $\sim 100$  Myr ago. The main dust component in the circumstellar envelope is solid iron. In these stars the poor formation of silicates is set by the strong nucleosynthesis experienced at the base of the envelope, which provokes a scarcity of magnesium atoms and water molecules, required to the silicate formation. The importance of the present results to interpret the data from the incoming *James Webb Space Telescope* is also discussed.

*Keywords:* stars: AGB and post-AGB — stars: abundances — Magellanic Clouds

### 1. INTRODUCTION

The Large Magellanic Cloud (LMC) has been extensively used as laboratory to test stellar evolution theories and dust formation mechanisms, owing to its relative proximity ( $\sim 50$  Kpc, Feast 1999) and a low average reddening ( $E(B - V) \sim 0.075$ , Schlegel et al. 1998).

The evolved stellar population of the LMC have been observed by several surveys, the two most recent and complete being the Two Micron All-Sky Survey (Skrutskie et al. 2006) and the Surveying the Agents of a Galaxy's Evolution Survey (SAGE), with the *Spitzer* Space Telescope (Meixner et al. 2006). The availability of this robust body of observational data has allowed a full exploration of the main properties of stars evolving through the Asymptotic Giant Branch (hereafter AGB, Marigo et al. 1999, 2003) and to study the dust enrichment from stellar sources (Srinivasan et al. 2009; Riebel et al. 2012)

The development of updated AGB models, in which the evolution of the star is coupled to the description of dust formation in their wind (Ventura et al. 2012, 2014b; Nanni et al. 2013, 2014) opened the way to the characterization of the individual sources detected by the aforementioned surveys (Dell'Agli et al. 2014a, 2015) and to estimate the overall dust production rate by AGB stars currently evolving in the LMC (Schneider et al. 2014; Zhukovska & Henning 2013).

Among the various observations in the framework of the *Spitzer* space mission, the SAGE-Spec survey (Kemper et al. 2010) obtained with the Infrared Spectrograph (IRS) is particularly important, since the analysis of the whole spectral energy distribution (SED) offers the opportunity of determining the overall bolometric flux and the mineralogy of the dust present in the circumstellar envelope (Jones et al. 2014). The results from IRS have been recently used to deduce the fluxes of the AGB stars that will be detected by the MIRI camera, mounted onboard of the *James Webb Space Telescope* (JWST, e.g. Jones et al. 2017); the launch of the JWST will open the possibility of extending this research to other Local Group galaxies.

In this work we attempt to explain the peculiar SED exhibited by a small sample of evolved M-stars in the LMC, which cannot be explained within the commonly assumed framework, that silicates are the dominant dust species formed in the wind of M stars.

Our analysis is driven by the changes in the surface chemical composition of AGB stars, particularly the evolution of the surface abundance of the chemical species involved in the formation of the main dust compounds produced in the wind of M stars. Based on the behaviour of silicon, magnesium and oxygen, we offer an innovative interpretation, suggesting that the dust in the circumstellar envelope of these objects corresponds to a rather unusual mineralogy, where solid iron is the dominant dust species.

The formation of dust mainly composed by solid iron particles in the winds of metal-poor, evolved stars finds support from independent observational evidences; McDonald et al. (2010, 2011) studied 14 metal-poor ( $[\text{Fe}/\text{H}] = -1.91$  dex to  $-0.98$  dex) giant stars (including AGB stars) in the Galactic globular cluster  $\omega$  Centauri and found that metallic iron dominates dust production in metal-poor, oxygen-rich stars; Kemper et al. (2002) found that metallic Fe is supposedly dominating the near-infrared flux of the M star OH 127.8+0.0. Taken together, theory and observations seem to create a picture where metallic Fe is a natural constituent of AGB winds. Our results in this Letter seem to reinforce this picture.

The conditions required to produce such a peculiar dust composition are achieved only by stars within a narrow range of ages and metallicities; therefore, the results presented here, if confirmed, can be used as an independent identifier of chemical composition and formation epoch of the sources observed. These findings will be important for the analysis of the soon-to-be results from the JWST mission, particularly when studying galaxies dominated by a metal poor stellar component.

## 2. IRON DUSTY AGB STARS IN THE LMC

In a recent work Jones et al. (2017) analyzed the SED of evolved stars in the LMC observed within the SAGE-Spec survey and provided the magnitudes expected in the mid-IR bands of the MIRI camera of the JWST.

Fig. 1 shows the distribution of the M stars analyzed by Jones et al. (2017) in the colour-magnitude ( $[7.7] - [25]$ ,  $[7.7]$ ) plane (hereafter CMD). The position of the stars in this plane allows the best discrimination of the mineralogy of the dust present in the circumstellar envelope, as the relative distribution of the various dust species mostly affects the details of the shape of the SED in the region covered by the MIRI filter centered at  $7.7\mu\text{m}$ .

Here we focus on the group of stars populating the left region of the CMD, located at  $[7.7] - [25] \sim 1.4$ ,  $[7.7] \sim 7.5 - 8$ , not covered by the tracks of  $Z = 8 \times 10^{-3}$  stars. These objects, indicated with blue squares in Fig. 1, exhibit a very peculiar SED; Fig. 2 displays three illustrative examples. The  $9.7\mu\text{m}$  feature in the SED indicates the presence of silicate type dust. On the other hand, the steep rise of the SED for wavelengths shorter than  $8\mu\text{m}$  cannot be reproduced if we assume that most of the dust is composed of silicates. This is shown in the middle panel of Fig. 2, where we report the SED obtained assuming the same luminosity of the best-fit model, an optical depth chosen to reproduce the morphology of the silicate feature, and iron-free dust: the comparison with the observed SED clearly shows that the overall SED, both in the spectral region  $\lambda < 8\mu\text{m}$  and at the mid-IR wavelengths  $\lambda > 12\mu\text{m}$ , does not match the observations.

Before presenting our interpretation on the evolutionary status of these objects, we briefly recall the most relevant physical and chemical properties of stars evolving through the AGB phase.

## 3. THE EVOLUTION THROUGH THE ASYMPTOTIC GIANT BRANCH

The AGB phase is experienced by all the stars of mass in the range  $0.8 M_{\odot} < M < 8 M_{\odot}$ . The pollution from these objects is associated to the changes in the surface chemical composition, caused by third dredge-up (TDU) and hot bottom burning (HBB). The former provokes a carbon enrichment of the surface regions, which can eventually lead to the formation of a carbon star (Iben 1974). HBB is related to the ignition of a p-capture nucleosynthesis at the

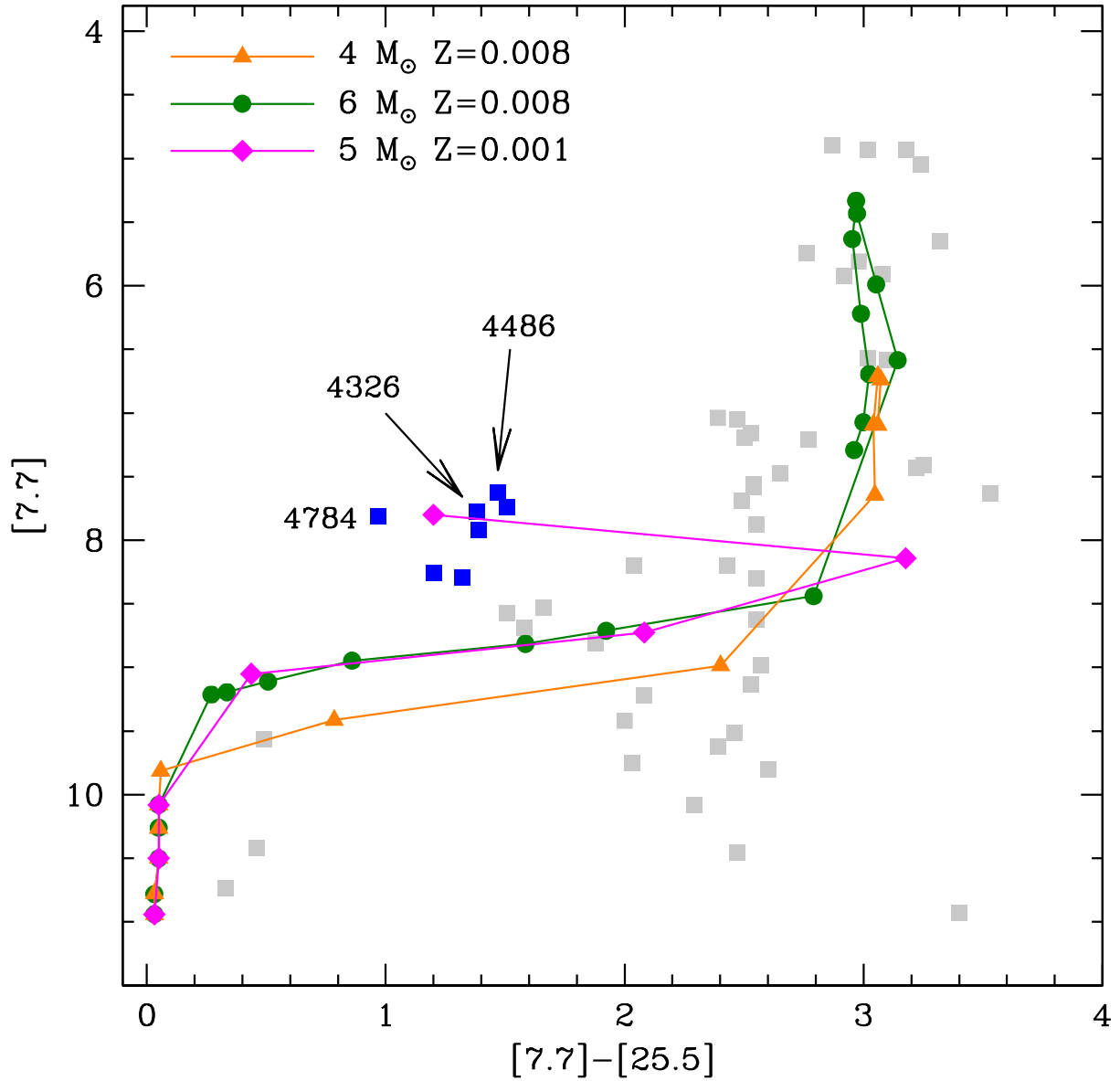


**Figure 1.** The distribution of the M-stars sample of the LMC analyzed by Jones et al. (2017), indicated by grey squares, in the color-magnitude ( $[7.7] - [25.5]$ ,  $[7.7]$ ) plane. Blue squares refer to the group of stars discussed in the present investigation. Green points and orange triangles indicate the synthetic colours assumed by stars of metallicity  $Z = 8 \times 10^{-3}$  and mass, respectively,  $4 M_{\odot}$  and  $6 M_{\odot}$ , during the AGB evolution. Magenta diamonds refer to the evolution of a  $5 M_{\odot}$  star of metallicity  $Z = 10^{-3}$ , before the achievement of the C-star stage.

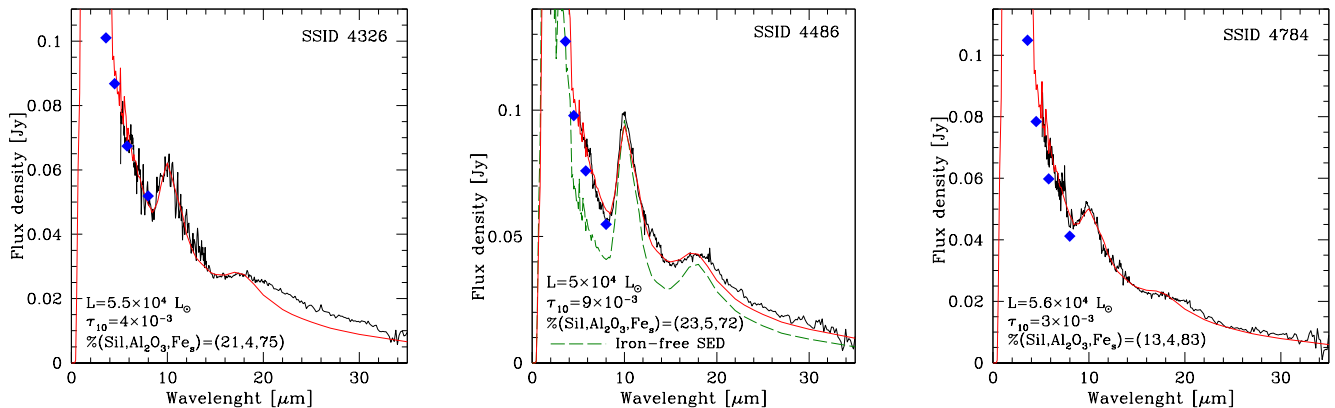


**Figure 2.** The comparison between the observed IRS spectra taken from Woods et al. (2011) (in black) and the synthetic SED (in red), obtained by assuming different luminosities and percentages of the various dust species, for three stars in the LMC, interpreted as low-metallicity massive AGBs (see text for discussion). Blue diamonds refer to IRAC [3.6], [4.5], [5.8], [8.0] photometry, from Meixner et al. (2006). The green, dashed line in the middle panel refers to a synthetic SED, calculated assuming iron-free dust around the star.

base of the convective envelope, when the temperature ( $T_{\text{bce}}$ ) exceeds  $\sim 30 - 40$  MK (Blöcker & Schönberner 1991); pollution from HBB reflects the equilibria of the p-capture reactions activated in the innermost layers of the envelope, which, in turn, are sensitive to  $T_{\text{bce}}$ .

### 3.1. Hot bottom burning in massive AGB stars

The ignition of HBB requires core masses above  $\sim 0.8 M_{\odot}$ , which reflects into initial masses  $M > 3 M_{\odot}$ . On general grounds, the higher the mass the stronger the HBB activated, because stars of higher mass evolve on bigger cores during the AGB phase. The strength of HBB is extremely sensitive to the metallicity, because lower  $Z$  stars attain hotter  $T_{\text{bce}}$ 's, thus experiencing a more advanced nucleosynthesis at the base of the envelope (Ventura et al. 2013). The description of HBB is highly sensitive to convection modelling (Ventura & D'Antona 2005), which is the reason for the significant differences obtained by the various groups studying AGB evolution.

Fig. 3 shows the evolution of the luminosity (left panel) and of the surface mass fractions of  $^{16}\text{O}$  and  $^{24}\text{Mg}$  (middle panel) of AGB stars of different mass and metallicity  $Z = 10^{-3}$ . The ignition of HBB is witnessed by the drop in the surface abundances of oxygen and magnesium, a signature of the activation of full CNO cycling and of the Mg-Al-Si nucleosynthesis. The strength of HBB is sensitive to the mass of the star: the  $4 M_{\odot}$  star experiences only a soft HBB, with the depletion of oxygen being limited to a factor of  $\sim 2$ , occurring only during the very late AGB phases. Conversely, in  $5 - 6 M_{\odot}$  stars, a significant depletion of both oxygen and magnesium takes place since the early AGB phases.

### 3.2. Dust formation in oxygen-rich AGB stars

The changes in the surface chemical composition reflects into the dust formed in the circumstellar envelopes of AGB stars. In the high-mass domain the effects of HBB provoke the destruction of the surface carbon, leaving no space for the formation of carbonaceous particles<sup>1</sup>. Under these conditions the most stable dust species are alumina dust ( $\text{Al}_2\text{O}_3$ ) and silicates. Solid iron particles also form, but in modest quantities, because this species is less stable than  $\text{Al}_2\text{O}_3$  and silicates, thus it forms in more external and less dense environments (Ferrarotti & Gail 2006).

$\text{Al}_2\text{O}_3$  forms in a region  $\sim 2$  stellar radii away from the photosphere of the star (Dell'Agli et al. 2014b); this very stable compound is extremely transparent to the electromagnetic radiation, thus its formation has negligible effects on the dynamics of the wind.

<sup>1</sup> This is connected with the high stability of the CO molecule (Sharp & Huebner 1990), which makes all residual carbon to be locked into CO in oxygen-rich stars

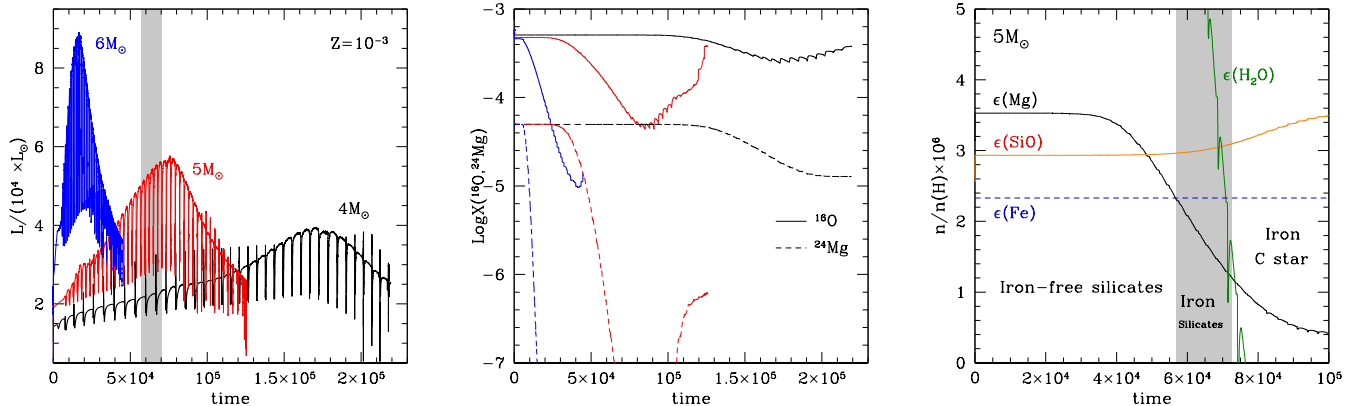


**Figure 3.** The variation of the main physical and chemical properties of stars of metallicity  $Z = 10^{-3}$  and initial mass  $4 M_\odot$  (black lines),  $5 M_\odot$  (red) and  $6 M_\odot$  (blue), during the AGB phase. Times on the abscissa are counted since the beginning of the thermally pulsating phase. The left and middle panels show, respectively, the variation of the luminosity and of the surface mass fractions of  $^{16}\text{O}$  (solid) and  $^{24}\text{Mg}$  (dashed). The right panel, which refers to the  $5 M_\odot$  model, shows the AGB variation of the main quantities relevant to dust production, namely the number densities of silicon (red, dashed) and water molecules (green), the latter being given by the oxygen excess with respect to carbon and silicon; all the four quantities are normalized to the number density of hydrogen. We mark the three AGB phases during which dust in the circumstellar envelope has the following composition: a) mainly silicates; b) a dominant solid iron contribution with traces of silicates and alumina dust; c) no silicates formation is possible, due to lack of water molecules. Grey shading in the left and right panels indicate the AGB phases of the  $5 M_\odot$  star corresponding to phase (b).

Among silicates, the most relevant species is olivine ( $\text{Mg}_2\text{SiO}_4$ ), which forms when the temperature of the gas drops below  $\sim 1100$  K, in a region of the circumstellar envelope located  $\sim 5 - 7$  stellar radii from the photosphere of the star. Formation of olivine particles occurs via a reaction involving SiO and water molecules and magnesium atoms; consequently, the amount of  $\text{Mg}_2\text{SiO}_4$  which can be formed is constrained by the number densities of silicon and magnesium, and by the excess of oxygen with respect to carbon and silicon (Ferrarotti & Gail 2006). As far as there are magnesium and oxygen available, silicates are the most abundant dust species, because the surface content of silicon and magnesium are higher than aluminium and iron.

The right panel of Fig. 3 shows the variation of the three aforementioned number densities and iron during the AGB evolution of the  $5 M_\odot$  star. All the quantities are normalized to the hydrogen density.

We can distinguish 4 phases.

1. In the initial AGB phases the surface magnesium is in excess of silicon, thus the rate of formation of silicates is constrained by the silicon abundance; in this regime the least abundant among the species involved in the formation reaction of olivine are the SiO molecules.
2. The ignition of HBB provokes the depletion of the surface Mg, thus the key species for the formation of silicates is magnesium; the dust formed is still dominated by silicates.
3. The action of HBB eventually makes the Mg/Fe ratio to drop below unity; in these conditions the formation of silicates is severely reduced, thus leaving room for the formation of solid iron dust.
4. During the final AGB phases the surface oxygen mass fraction becomes so small that the star becomes a C-star. The surface C is so low that iron dust is expected to be the dominant species anyway.

These results show that dust production in low- $Z$ , massive AGB stars can deviate from the common assumption that silicates is the dominant species, rather indicating that during the advanced AGB phases, after the effects of HBB have severely modified the surface chemical composition, there is wide room to the formation of iron grains.

Formation of metallic Fe in AGB atmospheres seems plausible from the expected condensation temperature (similar to that of silicates) at gas pressures typical of circumstellar environments (Gail & Sedlmayr 1999; Ferrarotti & Gail

2006). Laboratory experiments have shown that metallic Fe condenses almost ideally under high supersaturation conditions, and evaporates nearly ideally in vacuum (Tachibana et al. 2011). However, metallic Fe does not necessarily nucleate homogeneously in circumstellar environments, but likely through heterogeneous nucleation on pre-existing dust, e.g., the highly stable  $\text{Al}_2\text{O}_3$ . For a supersaturation ratio  $S > 1$ , the condensation and evaporation efficiencies are almost equal (Tachibana et al. 2011), which means that  $S > 1$  is in principle sufficient to grow metallic Fe. Thus, if silicate formation is suppressed due to low Mg abundance, metallic Fe can form and grow since efficient evaporation is essentially prevented in the presence of metallic iron vapour.

#### 4. DISCUSSION

In Fig. 1 we show two evolutionary AGB sequences, corresponding to stars of initial masses  $4 M_\odot$  and  $6 M_\odot$ , with  $Z = 8 \times 10^{-3}$  (Dell’Agli et al. 2015); this is the metallicity shared by the majority of the stars in the LMC younger than 200 Myr (Harris & Zaritsky 2009). The evolutionary paths in the figure can be explained by the significant production of silicates which starts after the beginning of HBB (Ventura et al. 2012; Dell’Agli et al. 2015). The tracks first move to the red, almost horizontally, owing to the gradual rise of the mid-IR flux as the circumstellar envelope becomes more and more opaque. The progressive increase in the rate of dust production eventually favours the formation of a prominent silicate emission feature at  $9.7\mu\text{m}$ , which lifts the flux in the  $7.7\mu\text{m}$  region, thus provoking a vertical upturn in the tracks.

Fig. 1 shows that the position of most M stars discussed by Jones et al. (2017) is reproduced by the evolutionary tracks: therefore, they can be explained within the traditional understanding, that dust formation around O-rich AGB stars is mainly composed by silicates, with little traces of alumina dust.

On the other hand, the colours and magnitudes of the peculiar stars, indicated with blue squares in Fig. 1, are not reproduced by the  $Z = 8 \times 10^{-3}$  tracks. As discussed in section 2 and shown in Fig. 2, their SED cannot be reproduced if we assume that silicates are the main dust species. We propose that the dust formed in the wind of these peculiar objects is mainly composed by iron grains. Indeed, Fig. 2 shows that a highly satisfactory fit of the observed SED is obtained by assuming  $\sim 70 - 80\%$  of solid iron, with smaller percentages of silicates ( $\sim 15 - 20\%$ ) and alumina dust ( $\sim 5\%$ ). We suggest that these stars descend from metal-poor progenitors with initial masses  $\sim 5 - 6 M_\odot$ , formed  $\sim 100$  Myr ago. The presence of a recent low-metallicity star formation activity is compatible with the star formation history and the age-metallicity evolution of the LMC computed by Harris & Zaritsky (2009). The particular mineralogy of the dust in the envelope of these objects is determined by the action of HBB, which, as described in the previous section, partly inhibits the production of silicates.

The evolutionary track of the  $5 M_\odot$  star discussed in Fig. 3 is shown in Fig. 1. During the first part of the evolution, corresponding to the phases (i) and (ii) above, the path followed is similar to the higher metallicity, massive AGBs: the track moves to the red, owing to the formation of silicates in the circumstellar envelope. However, when iron takes over as the dominant dust species (point iii above, grey-shaded region in Fig. 3) the track moves to the left, entering the region populated by the stars analyzed in the present investigation. According to these results, all the stars in the regions of the CMD at  $[7.7] < 7$  are massive AGBs of metallicity  $Z \geq 4 \times 10^{-3}$ .

Only low-metallicity stars of mass  $M > 4 M_\odot$  evolve through a phase dominated by iron dust, because the HBB experienced by lower mass objects is not sufficiently strong to trigger a significant decrease in the surface Mg and O (see middle panel of Fig. 3). The constraint on the initial mass is fully consistent with the luminosities required to reproduce the overall SED, of the order of  $50.000L_\odot$  (see grey-shaded areas in the left and right panels of Fig. 3). This interpretation is confirmed by the observed periods of the sources discussed, which are in the range 600 – 640 d (Fraser et al. 2008; Groenewegen & Sloan 2018): these are the same periods expected for the  $5 M_\odot$  star when evolving through the phase dominated by iron dust (grey-shaded regions in Fig. 3), calculated by applying eq. 4 in Vassiliadis & Wood (1993).

We rule out that the metallicity of the sources considered here is above  $Z > 2 \times 10^{-3}$ , because the HBB experienced is not sufficiently strong to allow a significant O and Mg depletion in the surface regions (Ventura et al. 2014a).  $Z \sim 10^{-3}$  represents the lowest metallicity that dust around M stars is currently observed to be forming at (Boyer et al. 2017).

The stars discussed here populate a specific region in the CMD; this opens the way to the definition of a criterion to identify metal-poor stars exposed to HBB in samples of AGB sources, which will be extremely important to interpret the data from the JWST space mission.

The inhibition of silicate production, which is related to the lack of magnesium, confirms that very low-metallicity, massive AGB stars experience strong HBB at the base of their envelope, thus suggesting that convection is extremely efficient in those physical conditions, far in excess of what is required to reproduce the evolution of the Sun.

## 5. CONCLUSIONS

We study a peculiar class of M-type AGB stars in the LMC, whose spectral energy distribution exhibits a peculiar shape, which cannot be explained by invoking a dominant contribution from silicates to the dust in the circumstellar envelope.

We propose that these sources descend from  $\sim 5 M_{\odot}$  stars,  $\sim 100$  Myr old, of metallicity  $Z \sim 1 - 2 \times 10^{-3}$ . The peculiar SED is due to the uncommon mineralogy of the dust in the circumstellar envelope, which is mainly ( $\sim 80\%$ ) composed by solid iron, completed by silicates and alumina dust particles. This distribution is favoured by the effects of hot bottom burning, which provokes a shortage of magnesium and water molecules, two essential ingredients for the formation of silicates.

Theoretical arguments show that gaseous iron is expected to condense efficiently in metallic iron in the winds of AGB stars; furthermore, there are observational evidences that iron grains are an important opacity source at low metallicities. However, this has been remained undetected for long, due to the iron featureless spectrum. In this work we have demonstrated the possibility of recognizing the presence of such iron grains from the observed SED of AGB stars.

This findings opens the way to use the incoming JWST observations to identify metal-poor, young stars, because these peculiar objects are expected to populate well identified regions in some of the colour - magnitude planes built with the MIRI filters. Side results of this study is the evidence that metal-poor, massive AGBs experience an advanced p-capture nucleosynthesis at the base of the envelope, a result still highly debated (see e.g. [Karakas & Lattanzio 2014](#)).

EM and PV are indebted to Franca D'Antona for helpful discussions. FDA and DAGH acknowledge support provided by the Spanish Ministry of Economy and Competitiveness (MINECO) under grant AYA-2017-88254-P.

## REFERENCES

- Blöcker T., Schönberner D., 1991, *A&A*, 244, L43
- Boyer M. L., McQuinn K. B. W., Groenewegen M. A. T., et al. 2017, *ApJ*, 851, 152
- Dell'Agli F., Ventura, P., García Hernández, D. A., et al. 2014a, *MNRAS*, 442, L38
- Dell'Agli F., García-Hernández D. A., Rossi C., et al. 2014b, *MNRAS*, 441, 1115
- Dell'Agli F., Ventura P., Schneider, R., et al. 2015, *MNRAS*, 447, 2992
- Feast M., 1999, *PASP*, 111, 775
- Ferrarotti A. S., Gail, H.-P. 2002, *A&A*, 382, 256
- Ferrarotti A. S., Gail, H.-P. 2006, *A&A*, 447, 553
- Fraser O. J., Hawley S. L., Cook K. H. 2008, *AJ*, 136, 1242
- Gail, H.-P. & Sedlmayr E. 1999, *A&A*, 347, 594
- Groenewegen M. A. T., Sloan, G. C. 2018, *A&A*, 609, A114
- Iben I. Jr. 1974, *ARA&A*, 12, 215
- Jones O. C., Kemper F., Srinivasan S., McDonald I., Sloan G. C., Zijlstra, A. A. A. 2014, *MNRAS*, 440, 631
- Jones O. C., Meixner M., Justtanont K., Glasse, A. 2017, *ApJ*, 841, 15
- Karakas A. I., Lattanzio, J. C. 2014, *PASA*, 31, e030
- Kemper F., de Koter A., Waters L. B. F. M., Bouwman J., Tielens A. G. G. M. 2002, *A&A*, 384, 585
- Kemper F., Woods P. M., Antoniou V., et al. 2010, *PASP*, 122, 683
- Marigo P., Girardi L., Bressan A. 1999, *A&A*, 344, 123
- Marigo P., Girardi L., Chiosi C. 2003, *A&A*, 403, 225
- McDonald I., Sloan G. C., Zijlstra A. A., et al. 2010, *ApJL*, 717, L92
- McDonald I., van Loon J. T., Sloan G. C., et al. 2011, *MNRAS*, 417, 20
- Meixner M. et al., 2006, *AJ*, 132, 2268
- Nanni A., Bressan A., Marigo P., Girardi, L. 2013, *MNRAS*, 434, 2390
- Nanni A., Bressan A., Marigo P., Girardi L. 2014, *MNRAS*, 438, 2328
- Riebel D., Srinivasan S., Sargent B., Meixner M., 2012, *ApJ*, 753, 71
- Schlegel D. J., Finkbeiner D. P., Davis M., 1998, *ApJ*, 500, 525
- Schneider R., Valiante R., Ventura P., et al. 2014, *MNRAS*, 442, 1440
- Sharp C. M., Huebner W. F. 1990, *ApJS*, 72, 417
- Skrutskie M. F., et al., 2006, *AJ*, 131, 1163
- Srinivasan S. et al., 2009, *AJ*, 137, 4810
- Tachibana et al., 2011, *ApJ*, 736, 16

- Vassiliadis E., Wood P. R. 1993, ApJ, 413, 641
- Ventura, P., D'Antona, F. 2005, A&A, 431, 279
- Ventura, P., Di Criscienzo M., Schneider R., et al. 2012, MNRAS, 420, 1442
- Ventura P., Di Criscienzo M., Carini R., D'Antona F. 2013, MNRAS, 431, 3642
- Ventura P., Di Criscienzo M., D'Antona F., Vesperini E., Tailo M., Dell'Agli F., D'Ercole A. 2014a, MNRAS, 437, 3274
- Ventura P., Dell'Agli F., Schneider R., et al. 2014b, MNRAS, 439, 977
- Woods P. M. Oliveira J. M., Kemper F., et al. 2011, MNRAS, 411, 1597
- Harris J., Zaritsky, D. 2009, AJ, 138, 1243
- Zhukovska S., Henning T. 2013, A&A, 555, A99